The Journal of Immunology

RESEARCH ARTICLE | MAY 15 2003

DNA Methylation and Chromatin Structure Regulate T Cell Perforin Gene Expression[1]

Qianjin Lu; ... et. al

J Immunol (2003) 170 (10): 5124–5132.
https://doi.org/10.4049/jimmunol.170.10.5124

DNA Methylation and Chromatin Structure Regulate T Cell Perforin Gene Expression[1]

Qianjin Lu,* Ailing Wu,* Donna Ray,* Chun Deng,† John Attwood,* Samir Hanash,* Matthew Pipkin,‡ Mathias Lichtenheld,‡ and Bruce Richardson[2]*§

Perforin is a cytotoxic effector molecule expressed in NK cells and a subset of T cells. The mechanisms regulating its expression are incompletely understood. We observed that DNA methylation inhibition could increase perforin expression in T cells, so we examined the methylation pattern and chromatin structure of the human perforin promoter and upstream enhancer in primary $CD4^+$ and $CD8^+$ T cells as well as in an NK cell line that expresses perforin, compared with fibroblasts, which do not express perforin. The entire region was nearly completely unmethylated in the NK cell line and largely methylated in fibroblasts. In contrast, only the core promoter was constitutively unmethylated in primary $CD4^+$ and $CD8^+$ cells, and expression was associated with hypomethylation of an area residing between the upstream enhancer at −1 kb and the distal promoter at −0.3 kb. Treating T cells with the DNA methyltransferase inhibitor 5-azacytidine selectively demethylated this area and increased perforin expression. Selective methylation of this region suppressed promoter function in transfection assays. Finally, perforin expression and hypomethylation were associated with localized sensitivity of the 5′ flank to DNase I digestion, indicating an accessible configuration. These results indicate that DNA methylation and chromatin structure participate in the regulation of perforin expression in T cells. ***The Journal of Immunology,*** **2003, 170: 5124–5132.**

DNA methylation is an essential element in differentiation during embryogenesis (1) and has been implicated in T cell differentiation as well. For example, changes in the methylation status and chromatin structure in the regulatory regions of the *IL-4* and *IL-13* genes are involved in the differentiation of Th2 cells (2), whereas similar changes affect the *IFN-γ* gene but not the *IL-4* and *IL-13* genes in Th1 cells (3). Other molecules selectively expressed in T cell subsets may similarly be regulated by DNA methylation and chromatin structure. To identify additional methylation sensitive genes, we performed oligonucleotide array analyses on T cells treated with the irreversible DNA methyltransferase inhibitor 5-azacytidine (5-azaC).[3] One transcript that reproducibly increased was perforin.

Perforin, encoded by the *PRF1* gene, is a pore-forming molecule expressed by cytotoxic lymphocytes and involved in immune mediated cell lysis. Perforin is expressed primarily in NK cells and effector $CD8^+$ T cells, and only in some $CD4^+$ T cell lines (4–7). Whereas IL-2 has been implicated in enhancing perforin expression through NF-κB and STAT5 signaling pathways and two enhancers (8, 9), additional control mechanisms must exist. For example, mice that are transgenic for the perforin promoter and upstream region express the promoter in all lineages physiologically able to express perforin irrespective of the expression status of the endogenous gene, implying negative control mechanisms not meditated by, but probably acting on, the promoter and flanking region (10). In the context of our observation of increased perforin levels in T cells treated with 5-azaC, we hypothesized that epigenetic mechanisms and chromatin structure might be involved in the regulation of perforin.

To test this hypothesis, we examined DNA methylation and chromatin structure of the perforin promoter and 5′ flanking sequences in primary T cells as well as in representative cell lines with differential perforin expression. We also determined how the methylation status affects the function of the perforin gene promoter. The results indicate an important role of DNA methylation and chromatin structure in regulating expression of this molecule in T lymphocyte subsets.

Materials and Methods

Cells and cell culture

The perforin-expressing SAM-19, derived from the mouse CTL/rat thymoma hybrid PC60, and human dermal and synovial fibroblasts, were cultured as previously described (8, 11). YT cells, a perforin-expressing NK cell line, were obtained from Dr. Y. Tagaya (National Cancer Institute, Bethesda, MD) and cultured in RPMI 1640 supplemented with 10% FCS, penicillin, and streptomycin. Human PBMC were isolated by density gradient centrifugation, and $CD4^+$ and $CD8^+$ T cells were isolated using Miltenyi beads and protocols provided by the manufacturer. Purity, assessed by flow cytometry, was typically >90%. Where indicated, purified T cells were stimulated with 1 μg/ml PHA for 24 h and then cultured with 1 μM 5-azaC (Sigma-Aldrich, St. Louis MO) in RPMI 1640/10% FCS/IL-2 for an additional 72 h. This protocol has been shown to be optimal for inducing expression of other methylation-sensitive T cell genes (12).

Oligonucleotide array analyses

RNA was isolated from untreated and 5-azaC-treated T cells and then analyzed using Affymetrix (Santa Clara, CA) U95A chips and protocols provided by the manufacturer. Results are presented as the mean ± SEM of two independent experiments.

*University of Michigan, Ann Arbor, MI 48109; †Astrazenica, Wilmington, DE 19850; ‡University of Miami, Miami, FL 33125; and §Ann Arbor Veterans Affairs Medical Center, Ann Arbor, MI 48109

Received for publication January 22, 2003. Accepted for publication March 6, 2003.

The costs of publication of this article were defrayed in part by the payment of page charges. This article must therefore be hereby marked *advertisement* in accordance with 18 U.S.C. Section 1734 solely to indicate this fact.

[1] This work was supported by Public Health Service Grants AG014783, AR42525, and AI42753; a Merit Grant from Department of Veterans Affairs (to B.R.); and Public Health Service Grant RO1CA055811 (to M.L.).

[2] Address correspondence and reprint requests to Dr. Bruce Richardson, 5310 Cancer Center and Geriatrics Center Building, University of Michigan, Ann Arbor, MI 48109-0940. E-mail address: brichard@umich.edu

[3] Abbreviations used in this paper: 5-azaC, 5-azacytidine; dC, deoxycytosine; d^mC, deoxymethylcytosine.

0022-1767/03/$02.00

Real time RT-PCR

Real time RT-PCR was performed using a LightCycler (Roche, Indianapolis, IN) and previously published protocols (13). The primers used to amplify the perforin transcripts were as follows: forward: 5′-CAC CCT CTG TGA AAA TGC CCT AC-3′; reverse: 5′-TCC AGT CGT TGC GGA TGC TAC-3′.

Results are expressed relative to β-actin transcripts measured as previously described (12). The identity of all amplified fragments was confirmed by melting curve analysis.

Flow cytometric analysis

PBMC or purified T cells were stained with anti-CD4-FITC and anti-CD8-CyChrome (BD PharMingen, San Diego, CA) and fixed with paraformaldehyde using previously published protocols (14). For perforin staining, CD4- and CD8-stained cells were permeabilized by suspension in 3 ml of 5% human serum/0.1% saponin/1% FBS/PBS followed by incubation at 4°C for 10 min in a light-protected vessel. The cells were then washed in 0.1% saponin/1% FBS/PBS, stained with anti-perforin-PE or a PE-conjugated isotype control (BD PharMingen) at 4°C for 30 min in 0.1% saponin/1% FBS/PBS, washed with the same buffer, suspended in 0.5 ml PBS, and then analyzed using a FACSCalibur (BD Biosciences, Franklin Lakes, NJ) flow cytometer and three-color analysis.

Bisulfite sequencing

Deoxycytosine (dC) and deoxymethylcytosine (d^mC) bases in the perforin gene promoter and 5′ flanking sequences were identified by bisulfite treatment of purified DNA (12) followed by nested PCR amplification of a 453-bp fragment located immediately 5′ to the perforin gene transcription start site (−457 to −4, containing the most proximal 17 CG pairs) and a more distal 679-bp fragment (−1326 to −599, containing 12 CG pairs). The primers were designed to account for the conversion of dC to deoxyuracil by the bisulfite, and *Eco*RI sites were added to the forward primers and *Xba*I to the reverse to facilitate cloning. The primers used were as follows: proximal first: forward: 5′-ATTGAATTCTAATTTTTAGGGTT TATATGATTTATAATTTT-3′; reverse: 5′-TCCTCTAGAAATAACAT CAACCCCCCAAACAACCCACTATAA-3′; proximal second: forward: 5′-AAGGAATTCAGGTATAGTGAGGTTGAAGAATTTTATTAGTTT-3′; reverse: 5′-TCCTCTAGACAACCACCACTCACATCACTTCTACTTC CTA-3′; distal first: forward: 5′-AGTGAATTCTGAAGTTGGGATTA GAATTTGTTTAGATTTTGT-3′; reverse: 5′-TAATCTAGAACCTA ACCCTTCTTAAATATCAAAACCTATAA-3′. distal second: forward: 5′-TTTGAATTCAGATATTTTGTAGGATTTTTATGTTTTTTAAAT-3′; reverse: 5′-TCTTCTAGACCACTTCCTACTCAACCTACATCCCACCCT AA-3′.

The amplified fragments were cloned, and five fragments were sequenced for each amplified region of each cell type as described (12).

DNase I sensitivity

DNase I-sensitive sites in the perforin gene promoter were identified as previously described (11). Briefly, nuclei were treated with 0, 40, 80, or 160 U/ml DNase I (Worthington Biochemical, Lakewood, NJ) at room temperature for 3 min. Then the reaction was stopped, and DNA was isolated, digested with *Eco*RI, fractionated by agarose gel electrophoresis, and transferred to nylon filters. The filters were hybridized with a 277-bp fragment excised with *Eco*RI and *Xba*I from a 1459-bp fragment encoding the perforin gene promoter and 5′ flanking region (−1400 to +59) previously described (8).

Patch methylation and cellular transfection

These studies used the previously described 1459-bp perforin gene promoter fragment (8) cloned into the *Eco*RI site of pGL3 (Promega, Madison, WI) containing a firefly luciferase reporter gene. *Nde*I and *Stu*I sites were engineered into the fragment at the indicated sites using the QuikChange site-directed mutagenesis kit (Stratagene, La Jolla, CA) as previously described (12). The regions of interest were excised using the appropriate restriction endonucleases, gel purified, methylated with *Sss*I and *S*-adenosylmethionine as described (12), and then religated back into the perforin gene-pGL3 construct. Controls included mock methylated constructs similarly generated but omitting the *Sss*I (12). Methylation was confirmed by digestion with *Aci*I. The methylated or mock methylated constructs were transfected into SAM-19 cells by electroporation using previously described protocols (12) and previously described β-galactosidase (12) or a *Renilla* luciferase expression construct (pRL-CMV; Promega) as transfection controls. Where indicated, recombinant murine IL-2 (Endogen, Woburn, MA) was added to SAM-19 cells at 1000 U/ml.

Statistical analysis

The significance of differences in the d^mC content of specific sequences was tested using a two-sided paired *t* test comparing the mean d^mC content of each CG pair within the sequence.

Results

Perforin protein and mRNA are induced by 5-azaC in primary T cell subsets

Preliminary studies used oligonucleotide arrays to identify T cell genes affected by DNA methylation inhibition. Purified T cells were stimulated with PHA for 24 h and then treated with the DNA methyltransferase inhibitor 5-azaC. Three days later gene expression was compared in treated and untreated cells using oligonucleotide arrays. Overall, 118 genes reproducibly increased 2-fold or more, and 12 decreased 2-fold or more. Of these, perforin expression was found to increase 4.3 fold ± 0.6-fold. To confirm these results, T cells were similarly stimulated with PHA and treated with 5-azaC. Three days later the cells were stained for perforin, CD4, and CD8 and analyzed by flow cytometry. Fig. 1*A* shows perforin expression in untreated $CD4^+$ T cells, whereas Fig. 1*B* shows perforin expression in 5-azaC-treated $CD4^+$ cells. The 5-azaC causes a modest increase in perforin expression. Fig. 1*C* shows that $CD8^+$ T cells express higher levels of perforin than $CD4^+$ cells as previously reported (15). The 5-azaC causes a further increase in perforin expression in these cells (Fig. 1*D*). Fig. 1*E* shows the level of perforin mRNA in PHA-stimulated $CD4^+$ and $CD8^+$ T cells similarly cultured with and without 5-azaC for 3 days, measured by real time RT-PCR and expressed relative to β-actin (mean ± SEM, $n = 3$). Because 5-azaC increased perforin mRNA, and as perforin mRNA is regulated at the transcriptional level (7), we addressed the possibility that demethylation of the perforin promoter and/or upstream enhancer participate in this process.

Perforin mRNA levels correlate with the methylation status and accessibility of the promoter and its 5′ flank

To this end we used cell line models representing perforin permissive vs unpermissive cell lines as well as primary, unstimulated $CD8^+$ T cells vs $CD4^+$ T cells. Initial experiments used real time RT-PCR to quantitate perforin mRNA levels in YT, an NK cell line that constitutively expresses perforin (16), and fibroblasts, which do not. Using β-actin as an internal standard, YT cells expressed 22.68 arbitrary units of perforin mRNA vs 0.0027 arbitrary units detected in a dermal fibroblast line and 0.00075 arbitrary units detected in a synovial fibroblast line. Perforin transcripts were then measured in $CD4^+$ and $CD8^+$ T cells. Freshly isolated $CD8^+$ T cells expressed ~7 times more perforin mRNA than did $CD4^+$ T cells (CD8 15.6 ± 3.49 (mean ± SEM, $n = 9$) vs CD4 1.93 ± 0.44 ($n = 10$), $p < 0.001$ by *t* test). This confirms differential perforin mRNA expression in YT cells relative to fibroblasts and freshly isolated $CD8^+$ T cells relative to CD4, and its correlation to perforin protein expression analyzed by FACS (Fig. 1, *A* and *C*), similar to a previous report (15).

Key elements of the human perforin gene promoter and 5′ flanking region are shown in Fig. 2*A*. The first 1300 bp 5′ to the transcription initiation site contains 29 potentially methylatable CG pairs. The first 55 bp 5′ to the start site contains a core promoter with a GC box. A series of repetitive elements is located between −396 and −83, and a region containing enhancer elements is located between −1136 and −983 (8, 17, 18). Relevant transcription factor binding sites are also shown. The methylation pattern of the region shown in Fig. 2*A* was then compared in YT cells and fibroblasts. DNA was isolated from YT cells and the two fibroblast lines, treated with bisulfite, and then the region shown in Fig. 2*A*

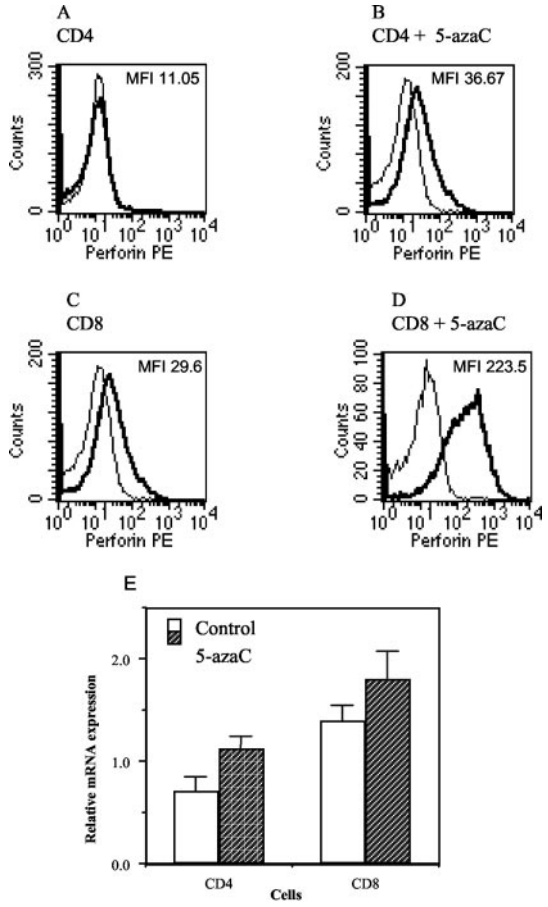

FIGURE 1. Perforin expression in 5-azaC-treated T cells. T cells were stimulated with PHA for 24 h, cultured alone or with 5-azaC for another 3 days, and then stained with anti-CD4-FITC, anti-CD8-CyChrome, and anti-perforin-PE or an isotype-matched control. *A*, Perforin expression in untreated $CD4^+$ T cells. The heavy line represents anti-perforin-PE, whereas the lighter line represents the isotype control. The mean fluorescence intensity of the perforin staining is shown. *B*, Perforin expression in 5-azaC-treated $CD4^+$ T cells, presented as in *A*. *C*, Perforin expression in $CD8^+$ T cells, presented as in *A*. *D*, Perforin expression in 5-azaC-treated $CD8^+$ T cells, presented as in A. *E*, PHA-stimulated and purified $CD4^+$ and $CD8^+$ T cells were treated with 5-azaC, and 3 days later perforin transcripts were measured relative to β-actin using real time RT-PCR. ■, Transcript levels in 5-azaC-treated cells; □, transcript levels in untreated cells. Results represent the mean ± SEM of three independent experiments using cells from three different donors.

was amplified in two fragments as described in *Materials and Methods*. The amplified fragments were cloned, and four to five independent clones per cell line were analyzed by sequencing. Fig. 2*B* shows the average of the 10 determinations for each CG pair in the two fibroblast lines, whereas Fig. 2*C* shows the average methylation of each CG pair for four to five fragments sequenced from the YT cells. The region is largely methylated in fibroblasts. In contrast, only a single methylated dC base was detected in perforin-expressing YT cells.

Fig. 2*D* shows the methylation of this region in $CD4^+$ T cells similarly determined using five clones for each of seven (bp −1326 to −599) or six (bp −457 to −4) healthy individuals, for a total of 35 or 30 fragments, respectively. The region from −1326 through the CG pair at −650 is relatively heavily methylated, whereas the more proximal CG pairs become progressively less methylated the closer they are to the transcription start site, with most of the methylated residues in the proximal sequences located in the region containing repetitive elements (Fig. 2*A*). Fig. 2*E* shows the average methylation status of the same region in $CD8^+$ T cells isolated from five (bp −1326 to −599) and four (bp −457 to −4) healthy individuals, for a total of 25 and 20 independent clones, respectively. Overall, the entire region tends to be less methylated in $CD8^+$ T cells compared with $CD4^+$ cells (mean fraction methylated 0.23 vs 0.48, CD8 vs CD4, $p < 0.001$ by paired *t* test). The region from −1326 to −1000 is less methylated than the corresponding region in the $CD4^+$ T cells (0.89 vs 0.52 for the analyzed region, CD4 vs CD8, $p = 0.003$). The region from −1000 to −599 flanking the enhancer elements (Fig. 2*A*) is also significantly ($p = 0.001$) less methylated in $CD8^+$ T cells relative to $CD4^+$ T cells (mean fraction methylated 0.41 vs 0.71), although there is one exception at −720. The region from −457 to the transcription start site was also less methylated in the $CD8^+$ T cells (0.21 vs 0.07, CD4 vs CD8, $p < 0.001$).

The differences in methylation between the $CD4^+$ T cells and the $CD8^+$ T cells is largely on a clonal basis, i.e., most CG pairs within a given allele are either methylated or not. Fig. 3 compares representative methylation patterns of the most distal 12 CG pairs (−1300 to −600) in $CD4^+$ and $CD8^+$ cells from two healthy individuals. The methylation status of each CG pair in five cloned fragments from the $CD4^+$ T cells of one individual is shown in Fig. 3*A*, and from the $CD8^+$ cells of the same subject in Fig. 3*B*. The 12 CG pairs are completely methylated in all five clones from the $CD4^+$ cells, whereas three clones from the $CD8^+$ cells were largely demethylated, and two were more methylated (*B*). Similar results are also shown in DNA isolated from a second individual (Fig. 3, *C* and *D*). Similar clonality was also observed for the distal portion of the region from −600 to 0 (data not shown).

Chromatin structure near the perforin promoter was compared in YT cells, fibroblasts, and $CD4^+$ and $CD8^+$ T cells using DNase I digestion. Nuclei were isolated and digested with increasing amounts of DNase 1. Then, DNA was isolated, digested with *Eco*RI, and the fragments analyzed by Southern blotting, schematically shown in Fig. 4*A*. Fig. 4*B* shows two experiments, one comparing the results of YT cells vs fibroblasts and the other CD4 vs CD8 T cells. A 2.65-kb *Eco*RI-*Eco*RI fragment is seen in all cells. DNase I digestion of YT cells releases 1.2-, 0.6-, 0.5-, and 0.4-kb fragments. In contrast, fibroblast DNA is resistant to DNase I in this region. The same 1.2-kb fragment is seen in both $CD4^+$ and $CD8^+$ T cells; however, at the highest DNase 1 concentration tested, the ratio of the intensity of the 1.2:2.65-kb bands is 4-fold greater in the $CD8^+$ T cells relative to the $CD4^+$ population, indicating that the chromatin from the $CD8^+$ cells is relatively more susceptible to DNase I digestion. The smaller fragments also appear in the $CD8^+$ cells, but are only faintly visible in DNA from the $CD4^+$ cells. Again, the 0.6:2.65-kb band ratio is 4-fold greater in the $CD8^+$ cells relative to the $CD4^+$ cells at the highest DNase 1 concentration. Interestingly, in YT cells the ratio of the 0.6:1.2-kb fragments is 0.62, whereas the 0.6:1.2-kb band ratio in the $CD8^+$ T cells is 0.09, suggesting that the region containing the smaller fragments is less accessible to DNase 1 than the 1.2-kb site in $CD8^+$ T cells relative to YT cells. Similar results were seen in a confirming experiment for each comparison (data not shown). Fig. 4*C* maps the DNase I-sensitive sites relative to the perforin promoter. The 1.2-kb fragment corresponds to cleavage at bp −200, a region completely demethylated in $CD8^+$ T cells but partially methylated in $CD4^+$ T cells. The 0.4-, 0.5- and 0.6-kb fragments map to bp −1000, −900, and −800, respectively. The −1000 accessibility corresponds to the upstream enhancer shown in Fig. 2*A* (−1136 to −983), a region hypomethylated in $CD8^+$ T cells relative to CD4, and in YT cells relative to fibroblasts.

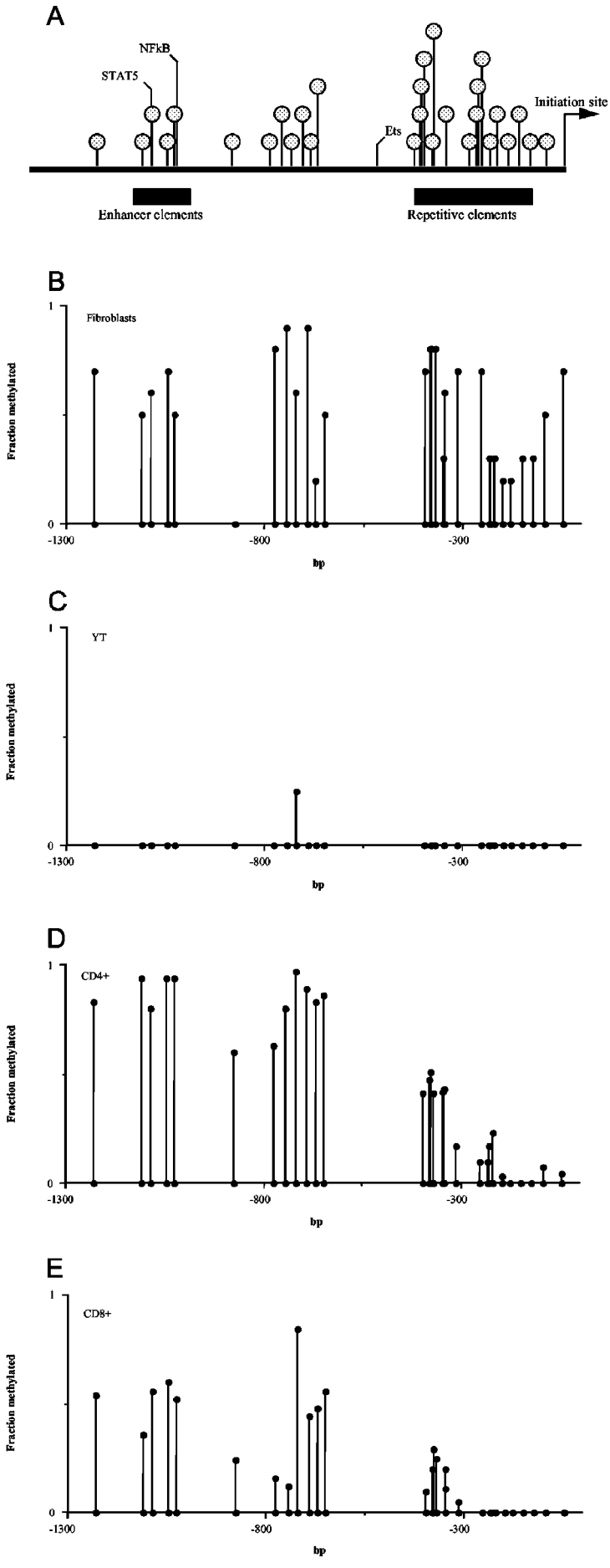

FIGURE 2. Methylation profile of the perforin gene promoter. *A*, The positions of the transcription initiation site, transcription factor binding sites, repetitive elements, and enhancer elements are identified. Each shaded circle identifies a potentially methylatable CG pair. *B*, DNA was isolated from two fibroblast lines and bisulfite treated. Then the region shown in Fig. 1 was amplified in two fragments (−1326 to −599 and −457 to −4). For each amplified fragment, five fragments from each line were cloned and sequenced. ● on the *x*-axis, each potentially methylatable CG pair; the height of the lines represent the mean fraction methylated of each dC base in these pairs, using 10 sequenced fragments from the two lines. *C*, DNA was isolated from YT cells, and the mean methylation of each CG pair was determined as in *B*. Results represent the mean of four determinations for the distal portion, and five determinations for the proximal portion. *D*, DNA was isolated from primary $CD4^+$ T cells, and the average methylation for each methylatable dC was determined as in *B*. Results represent the mean methylation of 35 fragments from seven donors (−1326 to −599) or 30 fragments from six donors (−457 to −4). *E*, DNA from primary $CD8^+$ T cells was analyzed as in *D*. Results represent the mean methylation of 30 fragments from six donors (−1326 to −599) or 25 fragments from five donors (−457 to −4).

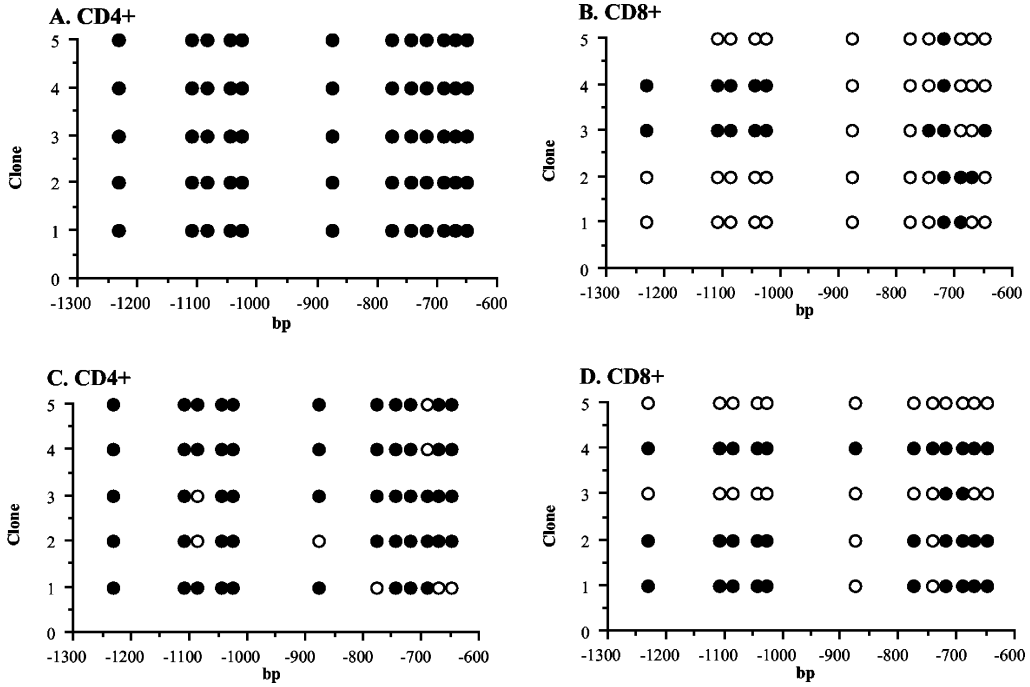

FIGURE 3. Methylation pattern clonality. ●, Methylated dC bases; ○, unmethylated bases. *A*, The figure shows the distal perforin promoter methylation pattern for each of the five cloned fragments from $CD4^+$ T cells of one of the donors shown in Fig. 2*C*. *B*, The methylation pattern of the five cloned fragments from $CD8^+$ T cells from the same individual shown in *A*. *C*, Methylation pattern of the same region in the five cloned fragments from $CD4^+$ T cells of a second individual. *D*, The methylation pattern of the five cloned fragments from $CD8^+$ T cells from the same individual shown in *C*.

5-azaC changes the methylation pattern of the perforin 5′ flank in primary T cell subsets, and regional methylation of the affected area reduces promoter activity

Fig. 5 shows the perforin gene methylation patterns in T cells from the same three donors shown in Fig. 1*E*, again sequencing five clones/donor. Fig. 5*A* shows the methylation pattern in untreated PHA-stimulated $CD4^+$ T cells, and Fig. 5*B* shows the pattern in the same cells treated with 5-azaC. 5-azaC had no significant effect on the methylation of CpG pairs between bp −1300 and −1000 (fraction methylated 0.67 vs 0.68, untreated vs treated, $p > 0.05$). In contrast, the region from −1000 to −600 containing the enhancer 3′ flanking region decreased the total fraction methylated (0.76 vs 0.48, untreated vs treated, $p = 0.006$). The most proximal region (−600 to 0) showed no significant decrease in the total fraction methylated (0.18 vs 0.17, untreated vs treated, $p > 0.05$). This suggests that demethylation of sequences linking the enhancer to the promoter may increase perforin expression in 5-azaC-treated $CD4^+$ T cells.

Fig. 5, *C* and *D*, similarly compare perforin gene promoter methylation in untreated and 5-azaC-treated $CD8^+$ T cells. As in the $CD4^+$ T cells, there was no significant difference in the methylation patterns in the region of −1300 to −1000. Also, the region from −1000 to −600 contained significantly less d^mC in the treated compared with the untreated cells (0.13 vs 0.33, $p = 0.02$). There was also a small but significant difference in the region from −600 to 0 (0.03 vs 0.08, $p = 0.008$). However, the effect of this small change in methylation status is uncertain. Together these results suggest that 5-azaC may increase perforin expression by demethylating sequences linking the enhancer to the promoter in $CD8^+$ T cells as well.

Fig. 5, *E* and *F*, show the clonal methylation patterns of the distal 12 CG pairs in untreated and 5-azaC-treated $CD4^+$ T cells from one of the individuals studied in Fig. 5, *A* and *B*. The distal region is nearly completely methylated in the PHA-stimulated $CD4^+$ T cells, similar to that observed in unstimulated cells (Fig. 3). The 5-azaC demethylated the region between −600 and −900 in three clones, whereas the more distal portion was demethylated in only one. Fig. 5, *G* and *H*, show similar studies in untreated and 5-azaC-treated $CD8^+$ T cells. Again, there is a preferential demethylation of the region between −600 and −900.

The functional effects of methylation on perforin gene promoter and enhancer function was tested using regional or "patch" methylation. These studies used a previously described 1459-bp fragment comprising the perforin promoter and upstream enhancer driving a firefly luciferase reporter gene (8). A *Nde*I site was engineered into the distal promoter at −290, and a *Stu*I site at −14. Transfection of the wild-type and mutated constructs into SAM-19 cells with β-galactosidase or *Renilla* controls demonstrated no significant effect on promoter function (luciferase:control ratios of 0.57 ± 0.15 vs 0.59 ± 0.20, wild type vs mutant, mean ± SEM of four experiments). The region from −1410 to −290 was then excised with *Eco*RI and *Nde*I, and the region from −1410 to −14 was excised with *Eco*RI and *Stu*I. The excised fragments were purified, methylated in vitro with *Sss*1 and S-adenosylmethionine, religated back into their respective reporter constructs, purified, and transfected into SAM-19 cells using a β-galactosidase or *Renilla* luciferase reporter constructs as a transfection control. Mock methylated constructs, similarly generated but omitting the *Sss*1, were applied as the comparison. Methylation of both regions inhibited promoter function, with methylation of −1410 to −14 giving slightly greater suppression (Fig. 6*A*). This suggests that the perforin gene promoter/enhancer fragment is methylation sensitive and that the methylation differences observed between YT cells and fibroblasts and between CD4 and $CD8^+$ T cells may be functionally significant. Further, hypomethylation of the core promoter appears to contribute little to expression if the remainder of the fragment is methylated.

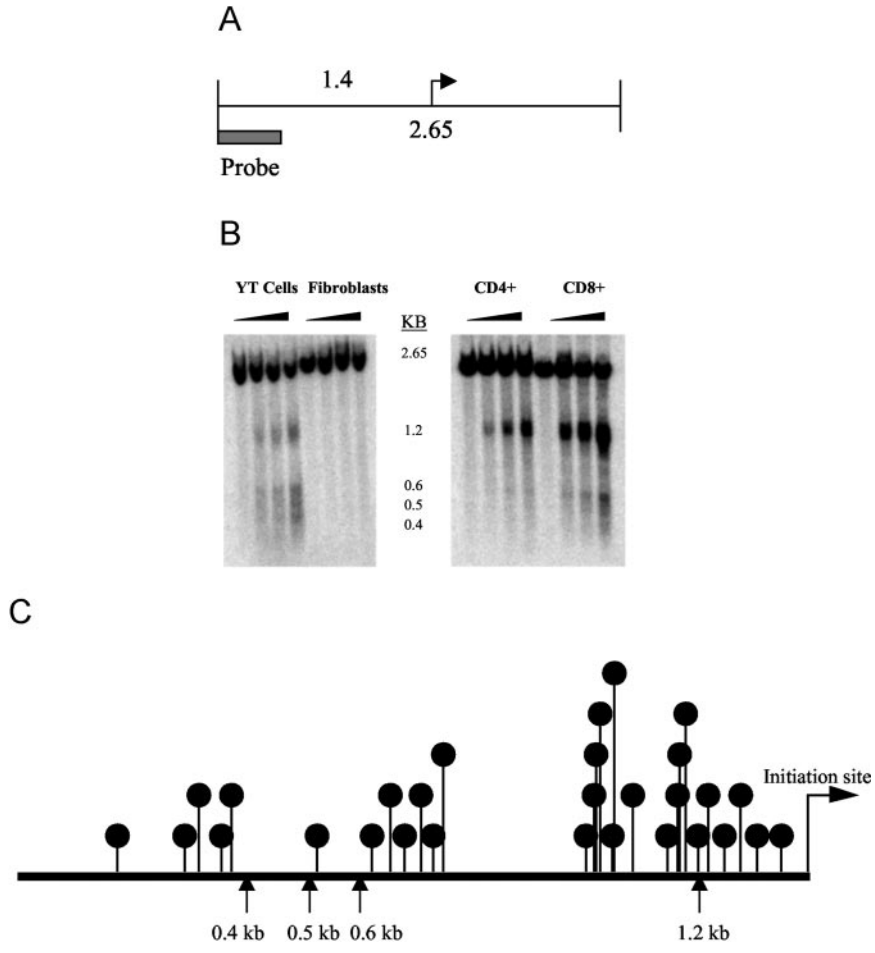

FIGURE 4. Perforin gene promoter chromatin structure. *A*, Map of the region analyzed, indicating the 2.65-kb *Eco*RI fragment, the transcription start site (arrow), and the location of the fragment used to probe the blot. The distance from the 5′ *Eco*RI site to the transcription start site is 1.4 kb. *B*, Nuclei were isolated from YT cells or fibroblasts (*left*), or $CD4^+$ and $CD8^+$ T cells (*right*). The chromatin was digested with 0, 40, 80, or 160 U/ml DNase I. Then Southern analysis was performed as described in *Materials and Methods*. Fragment size in kilobases is shown in the *middle* of the figure. *C*, The arrows identify cleavage sites producing the 1.2-, 0.6-, 0.5-, and 0.4-kb fragments shown in *B*. ●, CG pairs.

The functional effects of selectively methylating the enhancer flanking sequences was tested by patch methylation as before. An *Nde*I site was engineered at −979, and a *Stu*I site at −527. The region from −1410 to −979 was excised with *Eco*RI and *Nde*I, and the region from −979 to −527 with *Nde*I and *Stu*I. Both fragments were methylated in vitro, then methylated and mock methylated constructs were transfected into SAM-19 cells using *Renilla* luciferase as a control. Fig. 6*A* also shows that methylation of −979 to −527 decreased promoter function by ~70%. In contrast, methylating the 5′ flanking region (−1410 to −979) only decreased function by ~10%.

Previously, we reported that IL-2R signals can augment perforin expression, mediated by STAT5 and NF-κB and elements in the upstream enhancer region (8, 9). Hence, we tested whether signals from the IL-2R could overcome methylation-induced perforin gene suppression. Transfection of the perforin gene reporter constructs into SAM-19 cells with and without IL-2 demonstrated that IL-2 induced reporter activity 2.7-fold and 2.3-fold in two independent experiments, similar to our previous results (8). Methylated or mock methylated constructs were then transfected into untreated or IL-2-treated SAM-19 cells. Methylation of the region from −1410 to −14 as well as the region from −1410 to −290 completely inhibited IL-2-induced promoter function (Fig. 6*B*), indicating that IL-2 does not overcome inhibition by methylation.

Discussion

DNA methylation modifies gene expression through at least three mechanisms. Methylation of target sequences will prevent the binding of some transcription factors like AP-2, potentially suppressing expression (19). Methylcytosine binding proteins may also prevent the binding of transcription factors and can suppress gene expression from a distance (20). Methylcytosine binding proteins also attract chromatin remodeling complexes that modify adjacent histones, resulting in a condensed nucleosome structure inaccessible to transcription factors (21).

The studies described in this report indicate that DNA methylation and chromatin structure play a role in regulating perforin expression. Previous studies indicated that the perforin gene 5-flanking region contains a minimal promoter and an upstream IL-2-dependent enhancer (8, 17, 18). The present studies demonstrate that the proximal promoter region is relatively heavily methylated in nonpermissive fibroblasts, but constitutively demethylated in permissive YT cells and $CD4^+$ and $CD8^+$ primary T cells. However, expression was incomplete in both T cell subsets, with relatively less expression in the $CD4^+$ population. This is consistent with the relatively low expression observed in reporter constructs containing only the minimal promoter (8, 17) and also suggests that promoter hypomethylation is not sufficient for full gene expression.

In contrast to the promoter, the enhancer 3′ flanking region was significantly hypomethylated in $CD8^+$ T cells relative to $CD4^+$ cells, correlating with expression and suggesting that methylation of this region may suppress expression in the $CD4^+$ population. Interestingly, this area is also adjacent to an Ets element (bp −497) that is involved in the expression of perforin in NK cells via the transcription factor MEF (22). The reason for the differential methylation patterns in $CD4^+$ and $CD8^+$ T cells is unclear, but the patterns must be under the control of regulatory domains that are

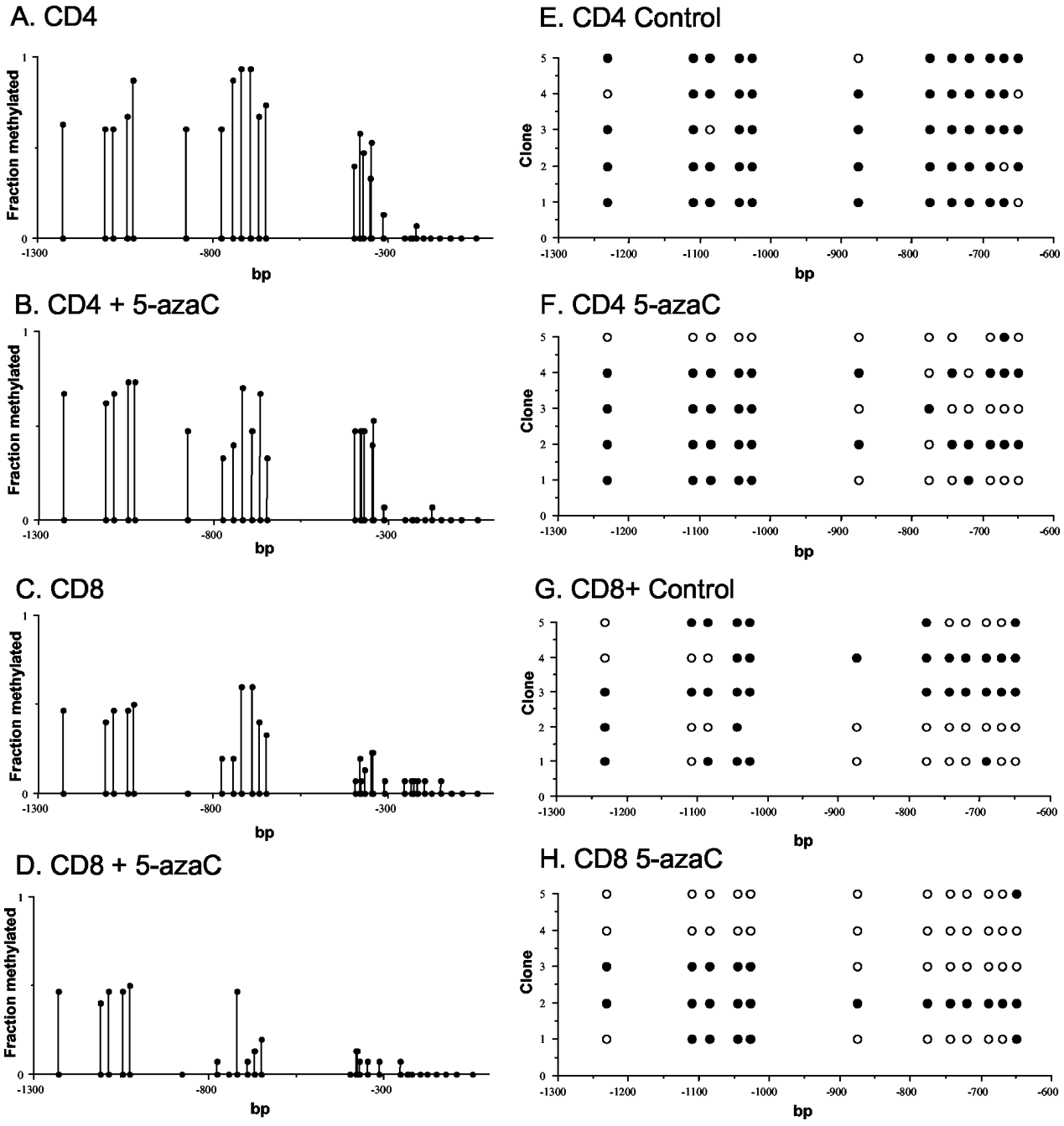

FIGURE 5. Effect of 5-azaC on perforin gene promoter methylation. *A*, DNA was isolated from the same three PHA-stimulated $CD4^+$ T cell lines shown in Fig. 1*E*, and methylation patterns were determined as in Fig. 2, sequencing five cloned fragments from each of the three lines. Results represent the mean fraction methylated of the 15 determinations. *B*, DNA was isolated from the same three PHA-stimulated, 5-azaC-treated $CD4^+$ T cell lines shown in Fig. 1*E*. Methylation patterns were determined as in *A*. *C*, Methylation patterns were determined in the same three PHA-stimulated $CD8^+$ T cells shown in Fig. 1*E*, using the approach described in *A*. *D*, Methylation patterns were determined in the same three PHA-stimulated, 5-azaC-treated $CD8^+$ T cells shown in Fig. 1*E*, using the approach described in *A*. *E*, The clonality of the methylation pattern in the distal 12 CG pairs is shown in five independent clones from $CD4^+$ cells isolated from one donor. ●, Methylated dC bases; ○, unmethylated dC bases. *F*, The methylation pattern of five clones derived from $CD4^+$, 5-azaC-treated T cells from the same cell line shown in *E* is shown. *G*, The clonality of the same region is shown, analyzed as in *E* using $CD8^+$ T cells from one donor. *H*, The cells shown in *G* were treated with 5-azaC, and clonality was analyzed as above.

not present in the analyzed DNA. Notably, clonal heterogeneity was observed both in perforin expression and perforin gene methylation in $CD8^+$ cells, suggesting that methylation may play a role in regulating perforin expression in the $CD8^+$ population as well. The relative effects of methylation on the function of the enhancer vs methylation of both the enhancer and promoter was tested by methylating both the enhancer and promoter elements or the region from −290 to the 5′ end of the 1410-bp fragment containing the enhancer and promoter. Almost complete suppression was observed when the enhancer and 3′ flanking region was methylated, with relatively little further suppression from methylating the promoter as well, suggesting that methylation of the region 5′ to the promoter plays a major role in suppressing gene expression in both the $CD4^+$ and $CD8^+$ populations. Further, IL-2 did not reverse suppression, suggesting that neither STAT5 nor NF-κB, which are activated by IL-2R signals and control the upstream enhancer (8,

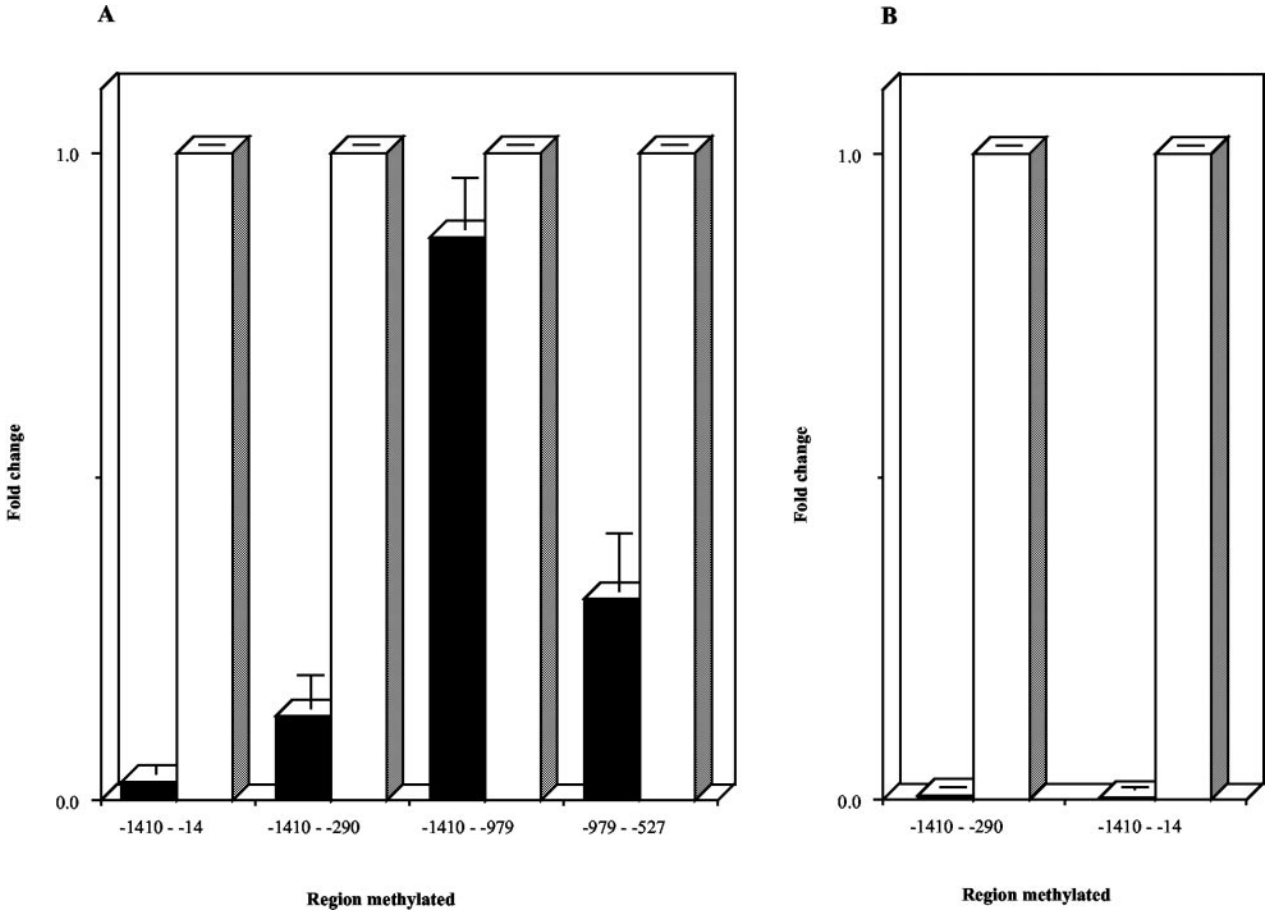

FIGURE 6. Effect of methylation on perforin gene promoter function. *A*, A 1459-bp perforin gene promoter fragment was cloned into a reporter construct containing a firefly luciferase reporter gene. The indicated regions, numbered as in Fig. 2*A*, were excised, methylated in vitro, religated into the reporter construct, and then transfected into SAM-19 cells. ■, Methylated construct; □, mock methylated constructs. Results are expressed relative to β-galactosidase or *Renilla* luciferase reporter constructs and are standardized to the mock methylated control. Results represent the mean ± SEM of four independent experiments for the first two data sets, and the mean ± SEM of two independent experiments for the second two data sets. *B*, The experiment shown in the first two data sets of *A* was performed in the presence of 1000 U/ml IL-2. Results are presented as in *A* and represent the mean ± SEM of two independent experiments.

9, 17), are able to overcome the methylation-dependent repressed state, at least in transient transfections.

The 5-azaC was used to further probe the role that DNA methylation plays in regulating perforin expression. The 5-azaC increased perforin expression at the protein and mRNA levels in both $CD4^+$ and $CD8^+$ T cells. Because 5-azaC is a DNA methylation inhibitor (23), this further argues that DNA methylation plays a role in regulating perforin expression in T cells. Bisulfite sequencing demonstrated that 5-azaC selectively decreases methylation of the enhancer 3′ flanking region in $CD4^+$ and $CD8^+$ T cells, suggesting that methylation of this region alone might be sufficient to suppress expression of the entire enhancer/promoter fragment. Regional methylation of the enhancer 3′ or 5′ flanking sequences confirmed that methylation of the 3′ sequences, but not the 5′, was sufficient to suppress expression. This suggests that the methylation status of the region linking the enhancer and promoter may have greater functional consequences on perforin expression than does methylation of the more 5′ region. Some methylcytosine binding proteins can suppress gene expression from a distance (20), and it is possible that methylation of the linking region suppresses both the promoter and enhancer more efficiently than methylation of more distant sequences.

Current evidence also indicates a prominent role of DNA methylation in directing the chromatin inactivation complexes to specific regions, causing chromatin condensation into a transcriptionally inactive complex, inaccessible to transcription factors (21). Although this mechanism is unlikely to contribute significantly to suppressing expression of the reporter constructs, it may well play a role in cells. The DNase I studies demonstrated that in fibroblasts, the entire perforin gene promoter/enhancer fragment was inaccessible to the enzyme, implying a condensed configuration. In contrast, DNase I cleaved in the enhancer and promoter regions in YT cells, consistent with a more open configuration at both sites. Similar studies in $CD4^+$ and $CD8^+$ T cells demonstrated that DNase 1 cleaved at the same site near the core promoter in both cell types, suggesting that the promoter was in an accessible configuration. The $CD4^+$ population was somewhat less susceptible to digestion at this site than the CD8, and the promoter flanking region was also more heavily methylated, suggesting that the methylation may have promoted condensation in some nonexpressing cells. However, the enhancer 3′ flanking region in the $CD4^+$ cells was almost completely resistant to digestion, although it was distinctly more susceptible in the CD8 cells. Similarly, the enhancer region in the YT cells was more sensitive to digestion than the $CD8^+$ cells. This correlates well with the methylation profiles and suggests that in YT and in some $CD8^+$ T cells the enhancer is in a more open configuration than in $CD4^+$ cells, accessible to DNase I as well as transcription factors, and that demethylation of the

flanking sequences may promote a more open configuration. In addition, formation of DNase I hypersensitive sites is an all or nothing phenomena and occurs on a clonal basis, similar to the methylation supporting this model.

In conclusion, perforin expression is increased in T cells following treatment with 5-azaC. This increase is associated with hypomethylation of the region residing between the upstream enhancer and the promoter in model cell lines. Methylation of this DNA suppresses promoter function, suggesting that methylation plays a role in regulating perforin expression in T cells. Also, the differential methylation patterns in the $CD4^+$ and $CD8^+$ subsets suggests that enhancer flanking region methylation is involved in the differential expression. Notably, this region is very well conserved with the mouse gene, and a part of it acts positively vs negatively in permissive vs unpermissive cells, (24) further highlighting the importance of this region. Our results are similar to those observed with specific cytokines associated with T cell differentiation (2, 3) and support the concept that DNA methylation plays a role in T cell differentiation. These results also suggest that perforin may be abnormally expressed in conditions associated with T cell DNA hypomethylation, such as lupus and aging (25, 26).

Acknowledgments

We thank Theresa Vidalon for her expert secretarial assistance.

References

1. Li, E., T. H. Bestor, and R. Jaenisch. 1992. Targeted mutation of the DNA methyltransferase gene results in embryonic lethality. *Cell 69:915.*
2. Santangelo, S., D. J. Cousins, N. E. Winkelmann, and D. Z. Staynov. 2002. DNA methylation changes at human Th2 cytokine genes coincide with DNase I hypersensitive site formation during $CD4^+$ T cell differentiation. *J. Immunol. 169: 1893.*
3. Agarwal, S., and A. Rao. 1998. Modulation of chromatin structure regulates cytokine gene expression during T cell differentiation. *Immunity 9:765.*
4. Hamann, D., P. A. Baars, M. H. Rep, B. Hooibrink, S. R. Kerkhof-Garde, M. R. Klein, and R. A. van Lier. 1997. Phenotypic and functional separation of memory and effector human $CD8^+$ T cells. *J. Exp. Med. 186:1407.*
5. Smyth, M. J., Y. Norihisa, and J. R. Ortaldo. 1992. Multiple cytolytic mechanisms displayed by activated human peripheral blood T cell subsets. *J. Immunol. 148:55.*
6. Richardson, B. C., T. Buckmaster, D. F. Keren, and K. J. Johnson. 1993. Evidence that macrophages are programmed to die after activating autologous, cloned, antigen-specific, $CD4^+$ T cells. *Eur. J. Immunol. 23:1450.*
7. Lichtenheld, M. G. 2000. Control of perforin gene expression: a paradigm for understanding cytotoxic lymphocytes? In *Cytotoxic Cells: Basic Mechanisms and Medical Applications.* M. V. Sitovsky and P. A. Henkart, eds. Lippincott Williams & Wilkins, Philadelphia, p. 123.
8. Zhang, J., I. Scordi, M. J. Smyth, and M. G. Lichtenheld. 1999. Interleukin 2 receptor signaling regulates the perforin gene through signal transducer and activator of transcription (Stat)5 activation of two enhancers. *J. Exp. Med. 190:1297.*
9. Zhou, J., J. Zhang, M. G. Lichtenheld, and G. G. Meadows. 2002. A role for NF-κB activation in perforin expression of NK cells upon IL-2 receptor signaling. *J. Immunol. 169:1319.*
10. Lichtenheld, M. G., E. R. Podack, and R. B. Levy. 1995. Transgenic control of perforin gene expression. Functional evidence for two separate control regions. *J. Immunol. 154:2153.*
11. Lu, Q., D. Ray, D. Gutsch, and B. Richardson. 2002. Effect of DNA methylation and chromatin structure on ITGAL expression. *Blood 99:4503.*
12. Lu, Q., M. Kaplan, D. Ray, S. Zacharek, D. Gutsch, and B. Richardson. 2002. Demethylation of ITGAL (CD11a) regulatory sequences in systemic lupus erythematosus. *Arthritis Rheum. 46:1282.*
13. Yung, R., D. Ray, J. K. Eisenbraun, C. Deng, J. Attwood, M. D. Eisenbraun, K. Johnson, R. A. Miller, S. Hanash, and B. Richardson. 2001. Unexpected effects of a heterozygous dnmt1 null mutation on age-dependent DNA hypomethylation and autoimmunity. *J. Gerontol. A Biol. Sci. Med. Sci. 56:B268.*
14. Richardson, B. C., J. R. Strahler, T. S. Pivirotto, J. Quddus, G. E. Bayliss, L. A. Gross, K. S. O'Rourke, D. Powers, S. M. Hanash, and M. A. Johnson. 1992. Phenotypic and functional similarities between 5-azacytidine-treated T cells and a T cell subset in patients with active systemic lupus erythematosus. *Arthritis Rheum. 35:647.*
15. Rukavina, D., G. Laskarin, G. Rubesa, N. Strbo, I. Bedenicki, D. Manestar, M. Glavas, S. E. Christmas, and E. R. Podack. 1998. Age-related decline of perforin expression in human cytotoxic T lymphocytes and natural killer cells. *Blood 92:2410.*
16. Yodoi, J., K. Teshigawara, T. Nikaido, K. Fukui, T. Noma, T. Honjo, M. Takigawa, M. Sasaki, N. Minato, M. Tsudo, et al. 1985. TCGF (IL 2)-receptor inducing factor(s). I. Regulation of IL 2 receptor on a natural killer-like cell line (YT cells). *J. Immunol. 134:1623.*
17. Yu, C. R., J. R. Ortaldo, R. E. Curiel, H. A. Young, S. K. Anderson, and P. Gosselin. 1999. Role of a STAT binding site in the regulation of the human perforin promoter. *J. Immunol. 162:2785.*
18. Lichtenheld, M. G., and E. R. Podack. 1989. Structure of the human perforin gene. A simple gene organization with interesting potential regulatory sequences. *J. Immunol. 143:4267.*
19. Comb, M., and H. M. Goodman. 1990. CpG methylation inhibits proenkephalin gene expression and binding of the transcription factor AP-2. *Nucleic Acids Res. 18:3975.*
20. Bird, A. P., and A. P. Wolffe. 1999. Methylation-induced repression—belts, braces, and chromatin. *Cell 99:451.*
21. Attwood, J. T., R. L. Yung, and B. C. Richardson. 2002. DNA methylation and the regulation of gene transcription. *Cell Mol. Life Sci. 59:241.*
22. Lacorazza, H. D., Y. Miyazaki, A. Di Cristofano, A. Deblasio, C. Hedvat, J. Zhang, C. Cordon-Cardo, S. Mao, P. P. Pandolfi, and S. D. Nimer. 2002. The ETS protein MEF plays a critical role in perforin gene expression and the development of natural killer and NK-T cells. *Immunity 17:437.*
23. Jones, P. A., S. M. Taylor, and V. L. Wilson. 1983. Inhibition of DNA methylation by 5-azacytidine. *Recent Res. Cancer Res. 84:202.*
24. Lichtenheld, M. G., and E. R. Podack. 1992. Structure and function of the murine perforin promoter and upstream region. Reciprocal gene activation or silencing in perforin positive and negative cells. *J. Immunol. 149:2619.*
25. Golbus, J., T. D. Palella, and B. C. Richardson. 1990. Quantitative changes in T cell DNA methylation occur during differentiation and ageing. *Eur. J. Immunol. 20:1869.*
26. Richardson, B., L. Scheinbart, J. Strahler, L. Gross, S. Hanash, and M. Johnson. 1990. Evidence for impaired T cell DNA methylation in systemic lupus erythematosus and rheumatoid arthritis. *Arthritis Rheum. 33:1665.*